EXPERIMENTAL STUDY OF MULTI-SCALE INTERACTION BETWEEN (INTERMEDIATE, SMALL)-SCALE MICROTURBULENCE AND MHD MODES IN EAST PLASMAS

P.J. SUN, Y.D. LI, X.D. ZHANG, G.J. WU, L.Q. XU, R. CHEN, H.L. ZHAO, J.Z. ZHANG, T.H. SHI, H.Q. LIU, Y.M. WANG, B. LYU, L.Q. HU, J. LI and the EAST team
Institute of Plasma Physics, Chinese Academy of Sciences
Hefei, China
Email: sunpj@ipp.cas.cn

Y. Ren
Princeton Plasma Physics Laboratory
Princeton, USA

Q. LI
Guangdong University of Technology
Guangzhou, China

Abstract

In this paper, we present evidence of multi-scale interactions between microturbulence and MHD modes in EAST core plasmas, including the first experimental identification of nonlinear coupling between microturbulence and an MHD mode during the current ramp-down phase in a set of L-mode plasmas in EAST and the effects of 2/1 classical tearing mode on microturbulence in the core of another set of EAST L mode plasmas. The microturbulence at different scales k = 10, 18 and 26 cm^{-1} (i.e., $k\rho_i \sim 2 - 6$. Here, ρ_i is ion gyroradius and k is the microturbulent wavenumber) was measured by the EAST tangential CO_2 laser collective scattering diagnostic in forward mode. We demonstrate the nonlinear coupling between microturbulence and MHD mode with bispectral analysis, showing statistically significant bicoherence correlated with the MHD mode. We also show that microturbulence spectral power is correlated to the 2/1 tearing mode and modulation effects on microturbulence by the 2/1 tearing mode.

1. INTRODUCTION

Measured electron thermal transport in magnetic fusion plasmas usually exceeds neo-classical expectations by one or more orders [1]. Microturbulence (especially for electron-scale one), coming from temperature and/or density gradient, is generally considered to be a major candidate in leading to such transport [2]. In addition to being driven by equilibrium plasma gradients, microturbulence can also be affected by its nonlinear interaction with macro-instabilities (e.g., neoclassical/classical tearing mode, kink mode, edge localized mode), either through nonlinear cascade process [3] or through equilibrium profile modulation by macro-instabilities. Perturbations from microturbulence and macro-instabilities may intrinsically exist in laboratory plasmas [4]. Multi-scale interaction inevitably occurs due to the simultaneous excitation of microturbulence and macro-instabilities during the long-pulse operation of high confinement plasmas, which is a crucial goal of current magnetic fusion research [5]. Multi-scale interaction between them can produces new phenomena (e.g., self-organization, the formation of regular structure), and thus, plasma anomalous transport can be affected. Therefore, understanding plasma transport in phases with significant MHD activities (especially during plasma current ramp-up/down and disruption) in tokamak plasmas is crucial for predicting and thus controlling plasma behavior for future fusion devices, e.g. ITER. Previous published papers mainly concentrated on studies of individual effects of microturbulence and macro-instabilities on plasma confinement and transport. But much less effort has been spent on the multi-scale interaction between them. According to the Ref. [6], microturbulence can be divided into three types, i.e., small-scale ($k\rho_i \geq 3$), intermediate-scale ($k\rho_i \sim 1 - 3$) and large-scale. In theories and simulations, the study of multi-scale nonlinear interaction between large-scale (low k) microturbulence and MHD mode have been reported in Refs. [7-9]. They found MHD modes can either directly or indirectly interact (through meso-scale structures such as zonal flows) with large-scale microturbulence. Due to the huge temporal and spatial scale separation between (intermediate, small)-scale microturbulence and macro-instabilities, it is impossible for the present-day supercomputers to simulate their nonlinear interactions in a self-consistent way. In experiments, several published papers show the multi-scale interaction between microturbulence and macro-instabilities. In TEXT tokamak, nonlinear coupling was observed between a long-wavelength mode (poloidal mode number m = 12. Here m is poloidal mode number) and large-scale ($\bar{k}_\theta = 3\ \mathrm{cm}^{-1}$, $\bar{k}_\theta \rho_i \sim 0.15$) microturbulence in edge plasmas [10]; the modulation relationship has been described between large-scale microturbulence and m/n=2/1 (n being toroidal mode number) tearing mode in the core

plasmas [11]. In DIII-D tokamak, localized modulation of large-scale $k_\theta < 1\,cm^{-1}$, $k_\theta\rho_i \sim 0.4$) microturbulence by NTM has been reported in [12,13]. In KSTAR tokamak, multi-scale interaction between large-scale ($k_\theta\rho_i \leq 0.4$) microturbulence and tearing mode has been demonstrated through a simultaneous two-dimensional measurements of the turbulence and poloidal flow profiles [14]. In HL-2A tokamak, cross-scale interactions among kink/ tearing modes and large-scale microturbulence have been studied [15]; Detailed study of the influence of m/n=2/1 magnetic island on perpendicular flows and large-scale microturbulence have been given in Ref. [16]. However, these experimental results mainly focus on the multi-scale interaction between large-scale microturbulence and MHD modes. As has been mentioned in Refs. [17-18], (intermediate, small)-scale microturbulence palys an important role in electron heat flux, and thus, the multi-scale interaction between (intermediate, small)-scale microturbulence and macro-instabilities inevitably affect the electron thermal transport (one of the unresolved central issues in magnetic fusion research). Thus how (intermediate, small)-scale microturbulence behaves when subjected to macro-instabilities is of great interest to study. In this paper, we present evidence of multi-scale interactions between (intermediate, small)-scale ($k\rho_i \sim 2-6$) microturbulence and MHD modes in EAST plasmas, including the first experimental identification of nonlinear coupling between microturbulence and an MHD mode during the current ramp-down phase in a set of L-mode plasmas in EAST and the effects of 2/1 classical tearing mode on microturbulence in the core of another set of EAST L mode plasmas using the EAST CO_2 laser collective scattering diagnostic in forward mode and far-forward mode.

2. EXPERIMENTAL SET-UP

Electromagnetic wave collective scattering is a powerful diagnostic to measure turbulent electron density fluatuations $\tilde{n}_e^2(\vec{k}, \omega)$ according to the relation $P_s \propto \tilde{n}_e^2$, when turbulent density fluctuation, scattered electromagnetic wave and incident electromagnetic wave satisfy energy conservation ($\omega = \omega_s - \omega_i$) and momentum conservation ($\vec{k} = \vec{k}_s - \vec{k}_i$). The scattering angle must satisfy the Bragg condition ($k = 2k_i \sin(\theta_s/2)$) due to $\omega_s \approx \omega_i$ and $k_s \approx k_i$. Figure 1 plots the schematic of EAST multi-channel tangential CO_2 laser collective scattering system used in the study of this paper. The main beam MB (laying in equatorial midplane EP; single mode TEM_{00}; input power $P_i \approx 10$ W) is usually used to produce scattered signals (focused to turbulent measurement region by a converging len CL0), and 'Local Oscillator' beams LO1-4 (all laying in the scattering plane SP) together with scattered signals are focused onto HgCdTe detectors through converging lenses CL1-4 (see figure 1). Note that the angle between SP and EP is 30^0 in this paper. This system can provide homodyne measurement of electron density fluctuations with frequency up to 1 MHz and with wave-number k ranging from 10 cm^{-1} to 30 cm^{-1}. The maximum scattering angle θ_s for our scattering system is less than 0.3^0. Due to the tangential scattering scheme employed in our experiment [19, 20], this scattering diagnostic can measure localized anisotropic density fluctuations with $\vec{k} \cdot \vec{B} \approx 0$ (k being the perpendicular wavenumber and B being local equilibrium magnetic field). The radial resolution for the diagnostic is $\Delta r = \pm 1$ cm, which is determined by the waist radius of the CO_2 laser beam (w ≈ 1 cm). This scattering diagnostic measures mostly radial wavenumber k_r, which is much larger than poloidal wavenumber k_θ. Although this diagnostic doesn't measure the modes with the highest saturated amplitude or the most unstable modes, we still believe the change of microturbulent power in this paper still can represent the overall change of microturbulent power. The wavenumber resolution is around 2 cm^{-1}. The scattering location and scattering volume for all the detection channels were calculated by a ray tracing code using an EFIT equilibrium reconstruction [21]. The scattering location is at $R_{sca} = 165.8$ cm ($\rho \approx 0.5$) on the high field side (HFS) for all the wave-numbers in this paper [22]. Low frequency coherent MHD modes, e.g. tearing mode, internal kink mode and energetic particle mode, can also be detected by this scattering diagnostic through the LO beam laser far-forward scattering mechanism [23, 24]. Moreover, the frequency of CO_2 laser is $f \approx 2.8 \times 10^{13}$ Hz, which is much larger than the electron plasma frequency ($f \sim 10^{10}$ Hz) in EAST. Therefore, no cut-off layer exists, and both

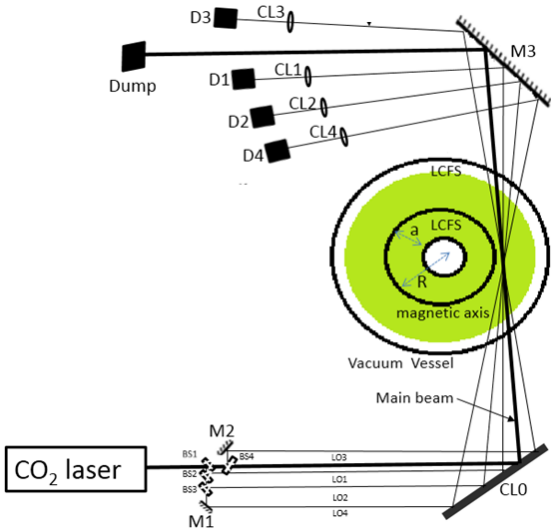

FIG. 1. A schematic of EAST multi-channel tangential CO_2 laser collective scattering diagnostic in the study presented in this paper, where 'D', 'LO', 'CL', 'M' and 'BS', represent detector, local oscillator, converging lens, mirror and beam splitter, separately; The angle between scattering plane (SP) and the equatorial midplane (EP) is 30°.

refraction and diffraction effects can also be negligible [20]. The wavenumber k of turbulent density fluctuations only depends on the corresponding scattering angle θ_s.

3. EXPERIMENTAL RESULTS AND DISCUSSION

As mentioned in previous paragraph, (intermediate, small)-scale ($k\rho_i \sim 2-6$) density fluctuations in the plasma core ($r/a \approx 0.5-0.6$) were measured through using the multi-channel tangential CO_2 laser collective scattering diagnostic. In the following section, experimental results will be presented to illustrate the multi-scale interaction between (intermediate, small)-scale microturbulence and macro-instabilities, which include the first experimental identification of nonlinear coupling between microturbulence and an MHD mode during the current ramp-down phase in a set of L-mode plasmas in EAST and the effects of 2/1 classical tearing mode on microturbulence in the core of another set of EAST L mode plasmas.

3.1. Experimental identification of nonlinear coupling between (intermediate, small)-scale microturbulence and an MHD mode

Here, we present the first experimental identification of nonlinear coupling between (intermediate, small)-scale microturbulence and an MHD mode in the core of EAST L mode plasmas. The observations were made during the plasma current ramp-down phase in a set of L mode deuterium plasmas with plasma current $I_p = 400$ kA and toroidal magnetic field $B_t = 2$ T. Note that both lower hybrid wave (LHW) and ion cyclotron range of frequency are turned off before the time range of interest $t = 8.2-9$ s. In the rest of this section, we will present results from a typical shot 42379 for which we have carried out extensive analysis.

The observation of the MHD mode is demonstrated in figure 2, which shows spectrograms of the signals from channel 1 of the collective scattering system (see figure 2(a)), a channel of soft x-ray measurements (see figure 2(b)) and a Mirnov coil (see figure 2(c)), separately. Only one harmonic can be seen in the soft x-ray signal and no harmonic can be seen in the Mirnov measurement, but multiple harmonics were observed in the collective scattering signal of channel 1 (note that all collective scattering channels detected this MHD mode with multiple harmonics). No harmonics in Mirnov measurement may be due to the magnetic fluctuation amplitude from the harmonics (corresponding to higher mode numbers) decrease faster versus radial coordinate r [12].

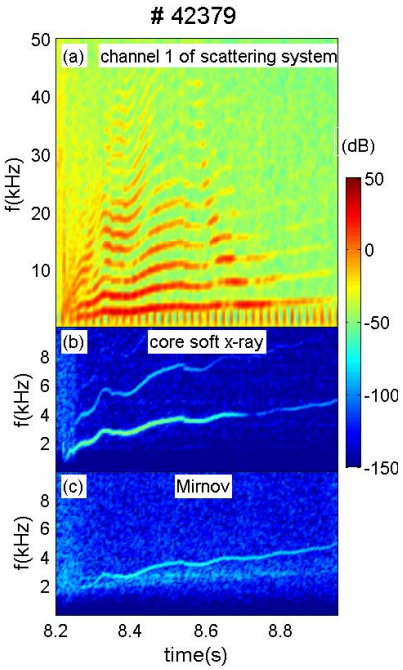

FIG. 2. Spectrograms of the signals from (a) channel 1 of the CO_2 laser collective scattering system, (f) a channel of soft x-ray measurements and (g) a Mirnov coil for the time range of interest (t = 8.2−9 s).

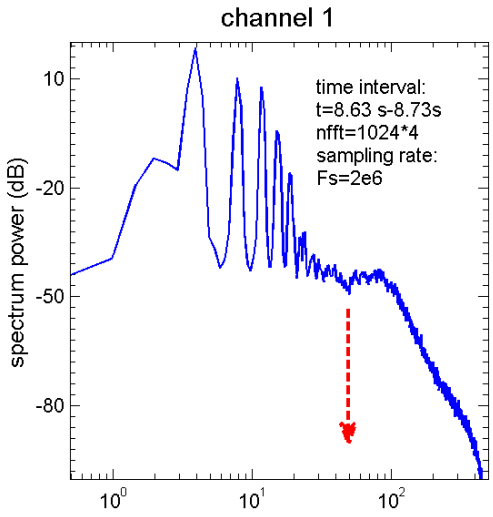

*FIG. 3. Power spectrum of channel 1 k = 10 cm^{-1} density fluctuation for the time t = 8.63s- 8.73 s with sampling rates 2MS/s and nfft=1024*4.*

Mode number of fundamental MHD mode has been identified as $m = -1$ and $n = 1$ through using mirnov coil arrays, and the fundamental frequency of this mode increases from 1 kHz to 4.8 kHz at $t = 8.2-9$ s (note that the 50 Hz bursting spikes at the bottom of figure 2(a) should be due to AC interference). In order to more clearly show the measurements of multiple harmonics of MHD mode and microturbulence, the power spectrum of channel 1 scattering signals for #42379 has been plotted in figure 3 for the time interval $t = 8.63-8.73$ s. The multiple harmonics from the MHD mode can be more clearly observed for the frequency $f < 50$kHz (from LO beam laser far-forward scattering signals). Broadband microturbulence from main beam CO_2 laser forward scattering mode can be identified at higher frequencies (f >

50 kHz). Microturbulent nature of higher frequency components is supported by a power-law fall-off at even higher frequencies, i.e. f > 80 kHz. Microturbulent power is much weaker than the MHD mode, as expected (small wavenumber features which have large power). Power reserval versus frequency f has been observed at the frequency $f \approx 50$ kHz, and this more clearly supports that f < 50 kHz scattering signals are from the MHD mode and f > 50 kHz ones are from brandband microturbulence. In the following contents, we will use bispectral analysis method [26] to identify the nonlinear interaction between (intermediate, small)-scale microturbulence and the MHD mode.

The bispectral analysis of channel 1 scattering signal is carried out for the time $t = 8.63 - 8.73$ s (see figure 4), when the power of both microturbulence and MHD mode are at quasi-steady state. Note that ensemble numbers is N = 200 (the noise level being 1/N = 0.05) and frequency resolution is $\Delta f = 1$ kHz. The spectral analysis is time averaged ($\Delta t = 1$ ms) over several fundamental MHD periods. As a function of frequencies f_1 and f_2, the squared autobicoherence $b^2(f_1, f_2)$ of channel 1 and channel 4 are plotted in figures 4(a) and (c) separately (here, (a) and (c) share the same colorbar). At the frequency $f_2 \approx -4$ kHz, significant squared autobicoherence can be found at $f_1 \approx 4$ kHz, 8 kHz, 16 kHz, 50 – 130 kHz for channel 1 ($k_1 = 10$ cm^{-1} density fluctuation) (see figure 4(a)) and at $f_1 \approx 4$ kHz, 8 kHz, 16 kHz, 100 – 300 kHz for channel 4 ($k_4 = 26$ cm^{-1} density fluctuation) (see figure 4(c)). These suggest that fundamental MHD mode couples with both its harmonics and microturbulence with $k = 10, 26$ cm^{-1} (similar results for $k_2 = 18$ cm^{-1} density fluctuation and not shown). In order to further investigate and better observe the nonlinear coupling between (intermediate, small)-scale microturbulence and the fundamental MHD mode, we fix the $f_3 = f_1 + f_2 = 4$ kHz, i.e. $f_2 = 4$ kHz$-f_1$. As a function of f_1, $b^2(f_1, 4\text{ kHz} - f_1)$ for channel 1 and channel 4 have been plotted in figure 4(b) and figure 4(d), separately. The

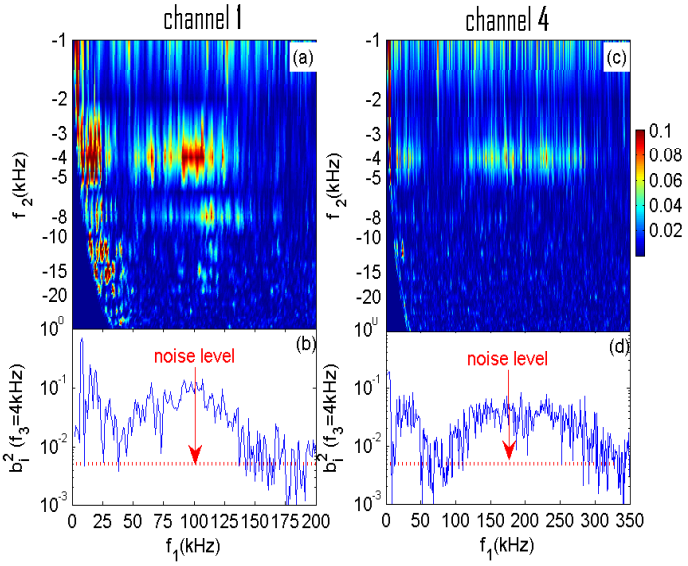

FIG. 4. (a) and (c): squared auto-bicoherence $b^2(f_1, f_2)$ of channel 1 density fluctuations and channel 4, respectively; note that panel (a) and (c) share the same colorbar. (b) and (d) squared auto-bicoherence $b^2(f_1, 4\,kHz - f_1)$ with f3 = 4 kHz (fundamental MHD mode frequency) for channel 1 and channel 4, respectively.

$b^2(f_1, 4\text{ kHz} - f_1)$ are much bigger than noise level in the frequency range $f_1 \sim 50 - 130$ kHz (see figure 4(b)) for $k_1 = 10$ cm^{-1} microturbulence. This suggests strong nonlinear coupling between the fundamental MHD mode with $f_3 \approx 4$ kHz and channel 1 microturbulence with frequency pairs $f_1 \sim 50 - 130$ kHz and 4 kHz$-f_1$. Similar results can also be found in figure 4(d), but the fundamental MHD mode is found to couple with higher frequencies of $k_4 = 26$ cm−1 microturbulence, i.e. $f_1 \sim 100 - 300$ kHz. It is also found that both mean frequency f_{mean} and spectral width δf for k_4 ($f_{mean} \approx 95$ kHz, δf ≈ 100 kHz) than k_1 ($f_{mean} \approx 73$ kHz, δf ≈ 75 kHz) microturbulence in the presence of MHD mode, where mean frequency f_{mean} is calculated using the expression $f_{mean} = \sum f S_k(f) / \sum S_k(f)$, and δf is from the full width at half maximum of the power spectrum. This result is also consistent with the theoretical results that microturbulence with higher wavenumber has higher corresponding real frequency and broader frequency spectral width. It is noted that bispectral analysis results can be affected by MHD mode, which can lead to a modulation of the Doppler shift of the microturbulence spectrum. The contents in the following will prove that the effect Doppler shift on bispectral analysis is limited. Both a similar MHD mode and $k_2 = 18$ cm^{-1} microturbulence (the angle between SP and EP is 0◦) have been measured simultaneously for another shot 41167 (not shown) by the scattering system. Ray tracing calculation shows that wavevector of k_2 microturbulence only contains radial wavenumber k_r. Therefore, Doppler shift should be 0 for k_2 microturbulence. But obvious bicoherence between the fundamental MHD mode (f ≈ 2.4 kHz) and $f \in [40, 90]$ kHz k_2 microturbulence also has been observed. So bicoherence results have been got in the absence of Doppler shift effect. Therefore, the effect of Doppler shift on bispectral analysis results is limited. This supports the validity of our bispectral analysis results on qualitatively identifying microturbulence-MHD mode nonlinear coupling in this paper.

3.2. Experimental study of the effect of 2/1 classical tearing mode on (intermediate, small)-scale microturbulence

In this section, we will present the study of the effects of 2/1 classical tearing mode on microturbulence in the core of another set of EAST L mode plasmas, which includes the modulation of both microturbulent mean frequency (Doppler shift effect) and microturbulent power (non-Doppler shift effect) by the 2/1 classical tearing mode.

A typical shot 43777 was selected, which has plasma current $I_p = 0.5$ MA, toroidal magnetic field $B_t = 2$ T, major radius $R_0 = 1.85$ m, and minor radius $a = 0.45$ m. Timings of interest are $t_1 = 3 - 3.6$ s and $t_2 = 6.38 - 7.5$ s when the central line-averaged electron density $\overline{n}_e(0)$, stored energy W_{dia} and poloidal beta β_p are nearly constant. The auxiliary heating is only LHW with the power $P_{LHW} \approx 1.2$ MW during the timings of interest. Spectrograms of density fluctuations from channel 1 ($k_1 = 10$ cm-1), channel 4 ($k_4 = 26$ cm^{-1}) and Mirnov signals have been plotted in figure 5(a) and figure 5(b) and figure 5(d), separately. Figure 5(c) plots the time evolution of Mirnov signal. Low-frequency tearing mode with fundamental frequency: f ~ 0.6 kHz at $t = t_1$ and f ~ 0.9 kHz at $t = t_2$) with at least two harmonics have been found in figure 5(d). Fundamental tearing modes' mode number have been identified as m/n=-2/-1 by Mirnov coils at both $t = t_1$ and $t = t_2$. According to the definition of the orientation of both I_p and B_t in ref. [27], these modes should rotate along electron diamagnetic drift direction in poloidal and counter-current direction in toroidal cross-section in the laboratory frame of reference, separately. At the time $t = t_2$, fundamental frequency of the tearing mode increases from f ~ 0 kHz at t ≈ 6.38 s to a f ~ 0.9 kHz at t ≈ 6.6−7.65 s, and then it evolves to f ~ 0 kHz at t ≈ 7.75 s. As mentioned before, microturbulent mean frequency f_{mean} can represent the lab frame frequency of microturbulence. f_{m1} and f_{m4} refer to the mean frequency of k_1 and k_4 microturbulence, and f_m is denoted by the black and white solid blocks in MHD-free phase and in tearing mode phase at $t = t_2$, separately (see figures 5(a) and (b)). From figure 5(a), we can see that k_1 microturbulent mean frequency increase from $f_{m1} = 31$ kHz at $t = 6.1 - 6.3$ s to $f_{m4} = 46$ kHz at $t = 7.1 - 7.3$ s (in the presence of tearing mode). Similar behavior has been observed for k_4 microturbulence, but its mean frequency increase more obvious than that of k_1, i.e., $f_{m4} = 35$ kHz to $f_{m4} = 62$ kHz. So both mean frequency itself and its increasing amount are a little bigger for k_4 microturbulence than k_1. Meanwhile, we also find that the temporal evolution of microturbulent mean frequency (not denoted in figures 5(a) and (b)) is almost consistent with that of fundamental tearing mode at $t = t_2$ (see figure 5(d)). Mode frequency can be described by $f_k = f_k' + k_t V_t/2\pi$ [28], where f_k and f_k' are mode frequency in the lab and plasma frame, separately. k_t, V_t are toroidal wavenumber of the mode and toroidal rotation velocity, respectively. $f_{Doppler} = k_t V_t/2\pi$ is the Doppler shift frequency. Usually, f_k' is much smaller than $f_{Doppler}$ and k_t is almost the same value, so we can find a a linear dependence relation between f_k and V_t. Figure 5(e) plots the time evolution of relative toroidal rotation velocity $\Delta V_t = V_t(t) - V_t(t = 2\ s)$ in central plasmas. ΔV_t was measured by a imaging x-ray crystal spectrometer diagnostic [29], which is based on the Doppler shift and broadening of line emission from trace amounts of highly ionized argon. A high anti-correlation relationship has been found between ΔV_t (or V_t) and k_1/k_4 microturbulent mean frequency (or frequency of fundamental tearing mode). This suggest that the increase of microturbulent mean frequency is greatly related to microturbulent Doppler shift $f_{Doppler}$. As mentioned before, toroidal wavenumber k_t of k_1/k_4

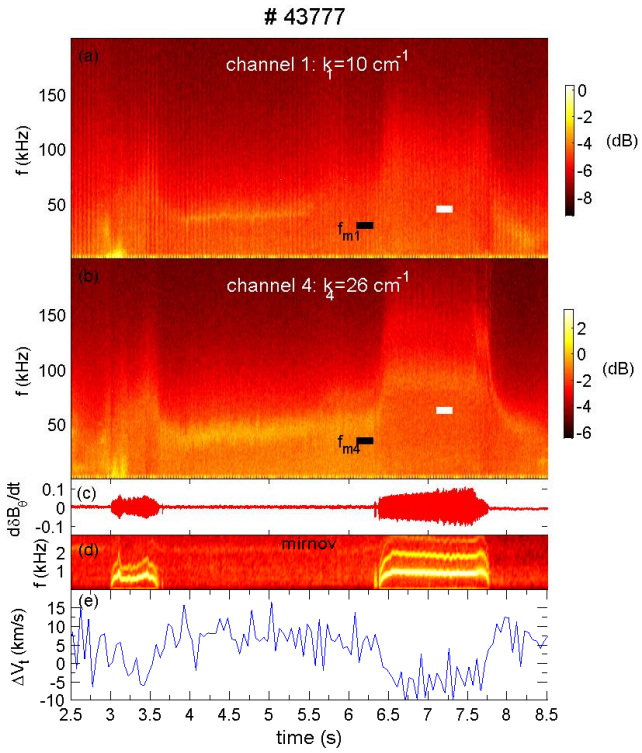

FIG. 5. Spectrograms of density fluctuations from (a) channel 1 ($k_1 = 10\ cm^{-1}$), (b) channel 4 ($k_4 = 26\ cm^{-1}$) and (d) Mirnov signals for t = 2.5–8.5 s; note that f_m denotes the mean frequency. (d) Time evolution of relative toroidal rotation velocity $\Delta V_t = V_t(t) - V_t(t = 2\ s)$ in central plasmas.

microturbulence and tearing mode is in the counter-current direction, i.e., $k_t < 0$. V_t is recognized as in the co-current direction ($V_t > 0$). So the Doppler shift for k_1/k_4 microturbulence and fundamental tearing mode satisfy $k_t V_t < 0$, which will give negative contribution to the frequency of both the k_1/k_4 microturbulence and fundamental tearing mode. Therefore, it is clear here that k_1/k_4 microturbulent mean frequency's increase is greatly related to the decrease of microturbulent Doppler shift due to the damping of toroidal velocity V_t by the 2/1 tearing mode.

Besides the modulation of microturbulent frequency by the 2/1 tearing mode through Doppler shift effect, microturbulent power also can be modulated through the modification of the equilibrium (non-Doppler shift effect) by the tearing mode. For the first step, we want to explore how microturbulent scattered power responds to the 2/1 tearing mode. For a given wavenumber k, density fluctuation frequency-integrated spectral power, S_{tot}, can reflect the scattered power of microturbulence [30]. Figure 6(a) and (b) plot the S_{tot} for $k_1 = 10$ cm^{-1} and $k_4 = 26$ cm^{-1} microturbulence with the time resolution $\Delta t = 50$ ms, separately. According to ref. [27], $\sqrt{\widetilde{B}_\theta(r_c)}$ is propotional to the magnetic island width, where $\widetilde{B}_\theta(r_c)$ is the amplitude of magnetic fluctuation at r_c, and r_c is the distance from toroidal magnetic center to the position of Mirnov coils. Here we define the relative width of magnetic island W as $W = \sqrt{\widetilde{B}_\theta(r_c)}$. Figure 6(c) plots the time evolution of W. At the time $t = 6.275 - 6.575$ s, S_{tot} for both $k_1 = 10$ cm^{-1} and $k_4 = 26$ cm^{-1} microturbulence increase as the time goes on. In the following time $t = 6.575 - 7.5$ s, S_{tot} for both $k_1 = 10$ cm^{-1} and $k_4 = 26$ cm^{-1} microturbulence decrease gradually, which are accompanied by the increase of W. These imply that scattered power from microturbulent is correlated with W. As we know that Doppler shift almost has little effect on the S_{tot} of microturbulence, so the initial increase and then decrease of k_1/k_4 microturbulent S_{tot} at $t = t_2$ should be from the modulation (non-Doppler) effect of tearing mode on microturbulence. Based on the above analysis, we will employ envelope and cross-correlation method to further analyze and verificate this. Envelope of density fluctuation signals can be calculated using either extracted extreme-value method or Hilbert transform method. We choose Hilbert transform method in the following analysis. The cross-power (see figures 6(d)) and squared coherence (see figures 6(e)) are carried out between Mirnov signals and the envelope of $k_4 = 26$ cm^{-1} density fluctuation. Figures 6(f) plot the cross-phase coefficient between $k_4 = 26$ cm^{-1} microturbulent envelope and Mirnov signals at the frequency of fundamental tearing mode. Here, these cross-correlation calculations have frequency resolution $\Delta f \approx 0.12$ kHz and N = 80 ensembles (noise level = 1/N = 0.0125). Figure 6(d) shows obvious power focuses on the frequency of fundamental tearing mode as well as its multiple harmonics, which demonstrates the modulation of $k_4 = 26$ cm^{-1} microturbulence by the 2/1 tearing mode. At the frequency of every cross-power peak (see figure 6(d)), the squared coherence value (see figure 6(e)) is much higher than the noise level (1/N = 0.0125). This supports that cross-power peaks (see figure 5(a)) are truly meaningful. The phase difference is nearly the same at the frequency of fundamental tearing mode for the time $t = t_2$. These results imply that the modulation of microturbulent power by tearing mode is continuous and the corss-correlation calculation is convergent. Similar results are got for both $k_1 = 10$ cm^{-1} and $k_2 = 18$ cm^{-1} density fluctuation, and they are not shown here.

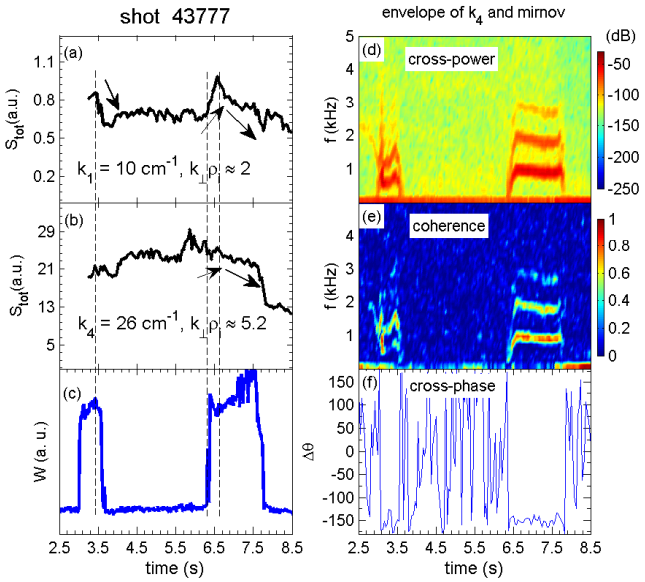

FIG. 6. Frequency-integrated spectral power S_{tot} of density fluctuation from (a) channel 1 ($k_1 = 10\ cm^{-1}$), (b) channel 4 ($k_4 = 26\ cm^{-1}$). (c) Time traces of the relative magnetic island width W, which is proportional to square root of the amplitude of magnetic fluctuations driven by 2/1 tearing mode; (d) The cross-power between Mirnov signal and the envelope of $k_1 = 10\ cm^{-1}$ density fluctuations. (e) The squared coherence between microturbulent ($k_1 = 10\ cm^{-1}$) envelope and Mirnov signal. (f) The cross-phase value between Mirnov signal and the envelope at the frequency of fundamental tearing mode. Note that frequency resolution is $\Delta f \approx 0.12$ kHz and ensembles are N = 80 (noise level: 1/N = 0.0125) for the calculations of cross-power, squared coherence and cross-phase (for full-band frequency).

4. SUMMARY

In summary, nonlinear coupling has been qualitatively identified for the first time between (intermediate, small)-scale microturbulence (k = 10, 18 and 26 cm^{-1}, $k\rho_i \sim 2-5.2$) and the MHD mode (m = −1, n = 1, f ≈ 4 kHz) through using bispectral analysis methodology. Statistically significant bicoherence has been observed between (intermediate, small)-scale broadband microturbulence and the MHD mode in the bispectral analysis for shot 42379. Similar results for #41167 support the validity of the results of qualitatively identifying microturbulence-MHD nonlinear coupling through using bispectral methodology (non-Doppler shift effect). Moreover, we also have carried out the study of the effect of 2/1 tearing mode on the (intermediate, small)-scale microturbulence in the core of an EAST L mode plasma discharge. The increase of k_1/k_4 microturbulent mean frequency is proved to be partly from the decrease of microturbulent Doppler shift due to 2/1 tearing mode. The obvious correlation between microturbulent S_{tot} and the width of magnetic island suggests the multi-scale interaction between microturbulence and the tearing mode. Cross-power, squared coherence and cross-phase results between microturbulent envelope and Mirnov signals further verificate modulation effects on microturbulent power by the tearing mode (beyond Doppler shift effect). Detailed study of the tearing mode modulation effect of both the equilibrium gradients (such as density gradient) and the $\vec{E} \times \vec{B}$ shearing rate on the microturbulence will be given in another paper.

ACKNOWLEDGEMENTS

The author thanks Prof W. X. Wang, Q. Q. Yu, J. Q. Dong, C. X. Yu, D. L. Brower, W. X. Ding, W. Chen, and Z. R. Wang for their useful discussions. This work has been supported by the National Natural Science Foundation of China with Contract Nos. 11475222, 11875286, 11505228, 11575238, 11575235, 11735016, National Key Development Project with Contract No. 2016YFA0400600, National Magnetic Confinement Fusion Science Program of China with Contract No. 2015GB101000 and the Science Foundation of ASIPP with Contact No. Y45ETY2307.

REFERENCES

[1] Wootton, A. J., et al., "Fluctuations and anomalous transport in tokamaks", Phys. Fluids B **2** (1990) 2879.
[2] Tang, W. M., "Microinstability theory in tokamaks", Nucl. Fusion **18** (1978) 1089.
[3] Pouquet, A., et al., "Strong MHD helical turbulence and the nonlinear dynamo effect", J. Fluid Mech. **77** (1976) 321.
[4] Yagi, M., et al., "Disparate Scale Nonlinear Interactions in Edge Turbulence", Contrib. Plasma Phys. **48** (2008) 13.
[5] Wang, Z. X., et al., "Magnetic-island-induced ion temperature gradient mode", Phys. Plasmas **103** (2009) 060703.
[6] Rhodes, T. L., et al., "Response of multiscale turbulence to electron cyclotron heating in the DIII-D tokamak", Phys. Plasmas **14** (2007) 056117.
[7] Ishizawa, A. and Nakajima, N., "Multi-scale-nonlinear interactions among micro-turbulence, double tearing instability and zonal flows", Nucl. Fusion **47** (2007) 1540.
[8] Li, J. Q., et al., "Finite frequency zonal flows in multi-scale plasma turbulence including resistive MHD and drift wave instabilities", Nucl. Fusion **49** (2009) 095007.
[9] Hornsby, W. A., et al., "The nonlinear coupling between gyroradius scale turbulence and mesoscale magnetic islands in fusion plasmas", Phys. Plasmas **17** (2010) 092301.
[10] Tsui, H. Y. W., et al., "Coherent nonlinear coupling between a long-wavelength mode and small-scale turbulence in the TEXT tokamak", Phys. Rev. Lett. **70** (1993) 2565.
[11] Yu, C. X., et al., "Tearing instabilities and microturbulence in TEXT", Nucl. Fusion **32** (1992) 9.
[12] Bardóczi, L., et al., "Modulation of Core Turbulent Density Fluctuations by Large-Scale Neoclassical Tearing Mode Islands in the DIII-D Tokamak", Phys. Rev. Lett. **116** (2016) 215001.
[13] Bardóczi, L., et al., "Multi-field/-scale interactions of turbulence with neoclassical tearing mode magnetic islands in the DIII-D tokamak", Phys. Plasmas **24** (2017) 056106.
[14] Choi, M. J., et al., "Multiscale interaction between a large scale magnetic island and small scale turbulence", Nucl. Fusion **57** (2017) 126058.
[15] Chen, W., et al., "Experimental observation of multi-scale interactions among kink /tearing modes and high-frequency fluctuations in the HL-2A core NBI plasmas", Nucl. Fusion **57** (2017) 114003.
[16] Jiang, M., et al., "Influence of m / n = 2/1 magnetic islands on perpendicular flows and turbulence in HL-2A Ohmic plasmas", Nucl. Fusion **58** (2017) 026002.

[17] Görler, T. and Jenko, F., "Scale Separation between Electron and Ion Thermal Transport", Phys. Rev. Lett. **100** (2008) 185002.

[18] Maeyama, S., et al., "Cross-Scale Interactions between Electron and Ion Scale Turbulence in a Tokamak Plasma", Phys. Rev. Lett. **114** (2015) 255002.

[19] Mazzucato, E., "Localized measurement of turbulent fluctuations in tokamaks with coherent scattering of electromagnetic waves", Phys. Plasmas **10** (2003) 753.

[20] Mazzucato, E., "Detection of short-scale turbulence in the next generation of tokamak burning plasma experiments", Plasma Phys. Control. Fusion **48** (2006) 1749.

[21] Lao, L. L., et al., "Reconstruction of current profile parameters and plasma shapes in tokamaks", Nucl. Fusion **11** (1985) 1611–22.

[22] Sun, P. J., et al., "Experimental study of the effect of 2/1 classical tearing mode on (intermediate, small)-scale microturbulence in the core of an EAST L mode plasma", Plasma Phys. Control. Fusion **60** (2018) 025019.

[23] Andel, H. W. H. V., et al., "Study of microturbulence in the TEXTOR Tokamak using CO_2 laser scattering", Plasma Phys. Control. Fusion **29** (1987) 49.

[24] Deng, C. B. and Brower D.L., "Far-forward collective scattering measurements of density fluctuations in the helically symmetric experiment stellarator", Rev. Sci. Instrum. **81** (2010) 10D503.

[25] Sun, P. J., et al., "Experimental identification of nonlinear coupling between (intermediate, small)-scale microturbulence and an MHD mode in the core of a superconducting tokamak", Nucl. Fusion **58** (2018) 016003.

[26] Kim, Y. C. and Powers, E. J., "Digital Bispectral Analysis and Its Applications to Nonlinear Wave Interactions", IEEE Trans. Plasma Sci. **PS-7** (1979) 120.

[27] Shi, T. H., et al., "Excitation of (2,1) neoclassical tearing modes by mode coupling with (1,1) internal mode in EAST", Plasma Phys. Control. Fusion **55** (2013) 055007.

[28] Ren, Y., et al., "Electron-scale turbulence spectra and plasma thermal transport responding to continuous $E \times B$ shear ramp-up in a spherical tokamak", Nucl. Fusion **53** (2013) 083007.

[29] Lu, B., et al., "Upgrades of the high resolution imaging x-ray crystal spectrometers on experimental advanced superconducting tokamak", Rev. Sci. Instrum. **83** (2012) 10E130.

[30] Mazzucato, E., et al., "Short-Scale Turbulent Fluctuations Driven by the Electron-Temperature Gradient in the National Spherical Torus Experiment", Phys. Rev. Lett. **101** (2008) 075001.